# We are IntechOpen,
# the world's leading publisher of
# Open Access books
# Built by scientists, for scientists

## 4,800
Open access books available

## 122,000
International authors and editors

## 135M
Downloads

Our authors are among the

## 154
Countries delivered to

## TOP 1%
most cited scientists

## 12.2%
Contributors from top 500 universities

## Interested in publishing with us?
## Contact book.department@intechopen.com

# Second Harmonic Generation under Strong Influence of Dispersion and Cubic Nonlinearity Effects

Sergey Mironov[1], Vladimir Lozhkarev[1], Vladislav Ginzburg[1],
Ivan Yakovlev[1], Grigory Luchinin[1], Efim Khazanov[1],
Alexander Sergeev[1], and Gerard Mourou[2]
*[1]Institute of Applied Physics, Nizhny Novgorod,*
*[2]Institut de la Lumière extrême (ILE), Palaiseau,*
*[1]Russia*
*[2]France*

## 1. Introduction

High intensity contrast ratio (ICR) is required for majority of experiments with strong-field radiation. The demands to temporal intensity profile are determined by task of application of super strong radiation. As a rule, the experiments require ICR as higher as possible. SHG process of powerful femtosecond radiation is known to be an excellent approach to significant enhancement of a temporal intensity profile. The peak power of output radiation of modern laser complexes exceeds the petawatt level (Aoyama, Yamakawa et al. 2003; Lozhkarev, Freidman et al. 2007; Liang, Leng et al. 2007 ; Yanovsky, Chvykov et al. 2008 ) and power density in the radiation is in a range of $10TW/cm^2$. At such high intensities cubic polarization of frequency doubling media is needed to be taken into consideration. The polarization leads to nonlinear phase accumulation of interacted waves (Razumikhina, Telegin et al. 1984; Choe, Banerjee et al. 1991; Chien, Korn et al. 1995; Ditmire, Rubenchik et al. 1996; Mironov, Lozhkarev et al. 2009) and small-scale self-focusing (SSSF) appearance (Bespalov and Talanov 1966; Rozanov and Smirnov 1980; Lowdermilk and Milam 1981; Kochetkova, Martyanov et al. 2009; Poteomkin, Martyanov et al. 2009). The present research is devoted to demonstration of a possibility of SHG process implementation for ICR enhancement.

In the chapter, we present theoretical and experimental results of SHG of output radiation of petawatt level femtosecond laser (Lozhkarev, Freidman et al. 2007). The influence of cubic polarization and dispersion effects are taken into account in the theoretical model. The coincidence of experimental results and the observed theoretical model are thoroughly discussed in section 2. Numerical simulation of SHG process has made it possible to demonstrate the possibility of ICR enhancement. We suggested a technique of additional pulse compression after SHG process. Results of the theoretical explorations are presented in section 3.

The model of linear stage of plane wave instability in media with quadratic and cubic nonlinearity is developed. The model is the generalization of the classical theory of beam

filamentation (Bespalov and Talanov 1966). Linear equations and methodic of their implementation for estimations of critical level of spatial noise in powerful laser beams are presented in section 4. We propose an original approach to small-scale self-focusing (SSSF) suppression in experiments with super intense radiation. The created theoretical model of the phenomena clearly explains the suppression, and its coincidence with an obtained experimental data is discussed in section 5. We present results of mathematical modeling of influence of surface dusts to generation of spatial noise and its further amplification during the SHG of super intense radiation.

## 2. Theoretical aspects and experimental results of SHG of super strong femtosecond radiation

SHG process of super intense femtosecond radiation in the frame of the second order of dispersion theory is described by the system of differential equations:

$$\frac{\partial A_1}{\partial z} + \frac{1}{u_1}\frac{\partial A_1}{\partial t} - \frac{ik_2^{(1)}}{2}\frac{\partial^2 A_1}{\partial t^2} = -i\beta \cdot A_1 A_2^* e^{-i\Delta kz} - i\gamma_{11}\left|A_1\right|^2 \cdot A_1 - i\gamma_{12}\left|A_2\right|^2 \cdot A_1$$

$$\frac{\partial A_2}{\partial z} + \frac{1}{u_2}\frac{\partial A_2}{\partial t} - \frac{ik_2^{(2)}}{2}\frac{\partial^2 A_1}{\partial t^2} = -i\beta \cdot A_1^2 e^{i\Delta kz} - i\gamma_{21}\left|A_1\right|^2 \cdot A_2 - i\gamma_{22}\left|A_2\right|^2 \cdot A_2, \tag{1}$$

where $A_1$ and $A_2$ are the complex amplitudes of the fundamental and the second harmonic fields, $z$ is the longitudinal coordinate of wave propagation, and $\Delta k = k(\omega_2) - 2k(\omega_1)$ is the linear wave vector phase mismatch, $u_1$ and $u_2$ group velocities of fundamental and second harmonic pulses, $\gamma_{ij}$ ($i,j$=1,2) are the coefficients of third-order nonlinear wave coupling. The inertia of cubic nonlinearity is not taken into consideration in the equations, because in our work we observe optical pulses with durations more than 5-10fs (Akhmanov, Vysloukh et al. 1988).

The cubic polarization of frequency doubling media leads to nonlinear phase (B-integral) accumulation of interacted fundamental and second harmonic waves. As a consequence of it, the waves acquire additional phase mismatch and the energy conversion efficiency decreases. We demonstrated in the frame of plane wave approximation (Mironov, Lozhkarev et al. 2009), that the detuning direction of fundamental beam propagation from phase matching angle on the amount (for oo-e type):

$$\Delta\theta = \frac{\Delta n}{n_1^3\left(n_1^{-2} - n_o^{-2}\right)}\sqrt{\frac{n_1^{-2} - n_o^{-2}}{n_e^{-2} - n_1^{-2}}}, \tag{2}$$

significantly        increases        energy        efficiency        significantly.        Here $\Delta n = \lambda A_{10}^2 \cdot \left(2\gamma_{11} + 2\gamma_{12} - \gamma_{21} - \gamma_{22}\right)/(8\pi)$, $n_1$ is the refractive index of an ordinary fundamental wave, $n_o$, $n_e$ are the main values of refractive indexes for the second harmonic, $A_{10}$ – amplitude of entrance to nonlinear element electric field. The detuning angle linearly depends on fundamental intensity, and for I=5 TW/cm$^2$ and 910nm central wavelength, the detuning angle in a KDP crystal is $\Delta\theta$=-0.5°.

The other important feature of SHG of femtosecond radiation is dispersion effects. As far as, refractive index of frequency doubling media depends on wave length, group velocities of fundamental and second harmonic waves are different. The fact is a cause of reducing area

of interaction of pulses. The phenomenon is characterized by the length of group velocities mismatch:

$$L_{12} = T \cdot \left| \frac{1}{u_1} - \frac{1}{u_2} \right|^{-1} = T \cdot P(\lambda),$$

here $T$ – is fundamental pulse duration, $P(\lambda)$ – dispersion parameter. Also, dispersion effects lead to pulse broadening. The spatial scale of the effect (the length of group velocity dispersion) can be found:

$$L_i = \frac{T^2}{4\ln(2)|D_i|}.$$

Here $D_i = \left. \dfrac{d^2 k}{d\omega^2} \right|_{\omega_i}$ ; $i=1$ for fundamental and $i=2$ for second harmonic. In order to decrease influence of the effects it is necessary to satisfy the conditions to the crystal length – $L$:

$$L_{nl} < L < L_{12}, L_1, L_2$$

here $L_{nl} = (\beta \cdot A_{10})^{-1}$ – typical scale of energy conversion to the second harmonic, $\beta$ – quadratic nonlinearity. Dispersion effects significantly depend on properties of frequency doubling media (at fundamental and second harmonic wave) and the fundamental pulse duration.

Experimental implementation of the SHG of femtosecond petawatt pulses requires a large aperture (more than 10cm) ultra-thin (hundreds of microns) nonlinear elements with wideband phase-matching at 800nm (Ti: sapphire lasers) and 910nm (optical parametrical amplification lasers). At present, KDP and DKDP crystals are the only crystals satisfying these requirements. Further analysis will be done for the crystals. We summarize characteristic lengths in Table.1.

| $\lambda_1$ nm | T=20fs | | | T=50fs | | | $T/L_{12}$, fs/mm | $L_{nl}$, mm (5TW/cm²) | Deuteration, level D |
|---|---|---|---|---|---|---|---|---|---|
| | $L_1$, mm | $L_2$, mm | $L_{12}$, mm | $L_1$, mm | $L_2$, mm | $L_{12}$, mm | | | |
| 800 | 5.3 | 1.36 | 0.26 | 33 | 8.52 | 0.65 | 77 | 0.15 | 0 |
| 910 | 12.7 | 1.65 | 0.55 | 79.4 | 10.4 | 1.38 | 36 | 0.18 | 0 |
| 800 | 4.06 | 1.34 | 0.21 | 25.38 | 8.38 | 0.52 | 97 | 0.15 | 1 |
| 910 | 6.02 | 1.62 | 0.33 | 30.76 | 10.14 | 0.82 | 61 | 0.18 | 1 |

Table 1. Characteristic lengths for KDP (D=0) and DKD crystals.

As can be seen from table 1, the effect of group velocities mismatch is more significant for SHG in comparison with the pulses broadening. The length of group velocity mismatch for 910nm fundamental wave length is two times more the one for 800nm. The difference is significant for super intense femtosecond radiation, because the mutual influence of cubic polarization and dispersion effects starts to be crucial. The efficiency of energy conversion vs KDP crystal length is presented in fig.1. The results were obtained in the assumption, that angle of beam propagation is optimal in accordance with formula (2).
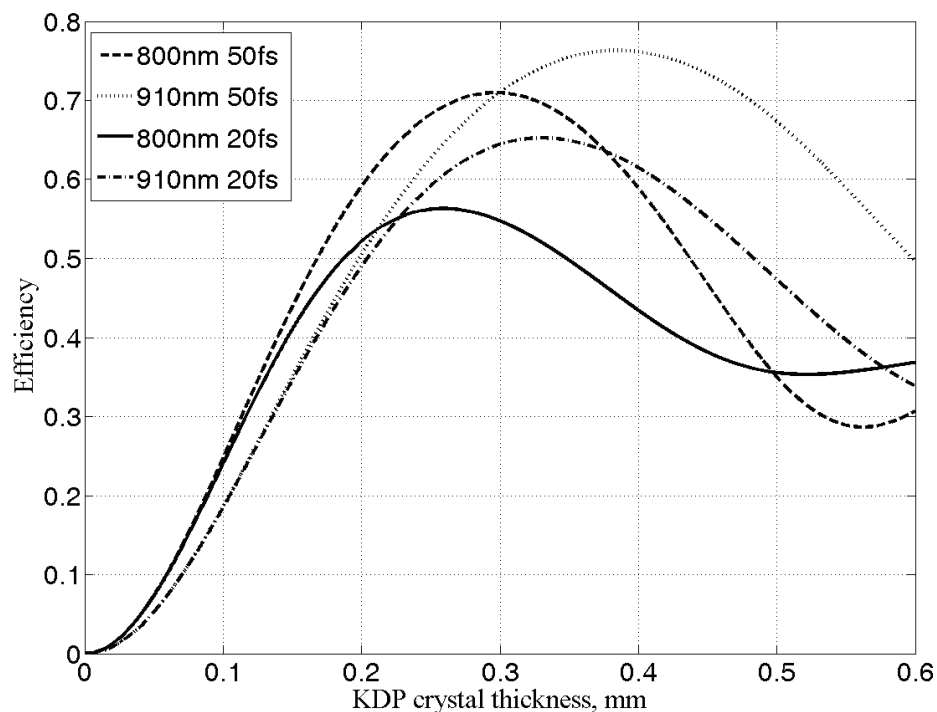
Fig. 1. The energy conversion efficiency vs KDP thickness, fundamental intensity 5TW/cm²

As can be seen from fig.1 optimal KDP crystal for effective SHG of 910nm, 50fs and I=5TW/cm² fundamental radiation is about 0.4mm, but the one for 800nm and the same parameters is about 0.3mm. The shorter pulses at the intensity level require thinner crystals. For instance, 20fs and 910nm the crystal length should be about 0.35mm, but for 800nm it is about 0.25mm. The right choice of nonlinear element thickness gives opportunity to obtain more than 50% efficiency of energy conversion even for 20fs, 5TW/cm² fundamental radiation in KDP crystal.

The length of group velocity mismatch can be varied by means of changing parameters of frequency doubling element. Deuteration factor – D in DKDP crystals can be chosen during their growth stage. Refractive index of the crystal depends on the deuteration factor, and hence group velocities of fundamental and second harmonic pulses can be varied. In fig.2 we present dependence dispersion parameter $P(\lambda)$ from fundamental wave length at different level of deuteration factor in DKDP crystal. We used DKDP properties from the work(Lozhkarev, Freidman et al. 2005).

According to fig.2, dispersion parameter $P(\lambda)$ (calculated for DKDP crystal) is equal to zero only for one fundamental wave length. In this case group velocities of fundamental and second harmonic pulses are equal. Evidently, the situation is optimal for frequency doubling process. For the deuteration factor D=0 (KDP crystal) optimal central wave length of fundamental pulse is 1033nm. The increasing of deuteration factor leads to optimal wave length varying. The D range 0 – 1 corresponds to diapason of optimal wave lengths 1033–1210 nm. So, the level variation of the deuteration can be used for managing of dispersion properties of frequency doubling nonlinear element. The dependence of refractive index for KDP and DKDP crystals from temperature can not be used for managing of dispersion properties. At the present, the crystals are optimal for SHG of super powerful ultra short laser pulses. As far as, created from the crystals nonlinear elements can be done with large

aperture (about 10 cm) and half millimeter thickness or less. The properties are crucial for the application.
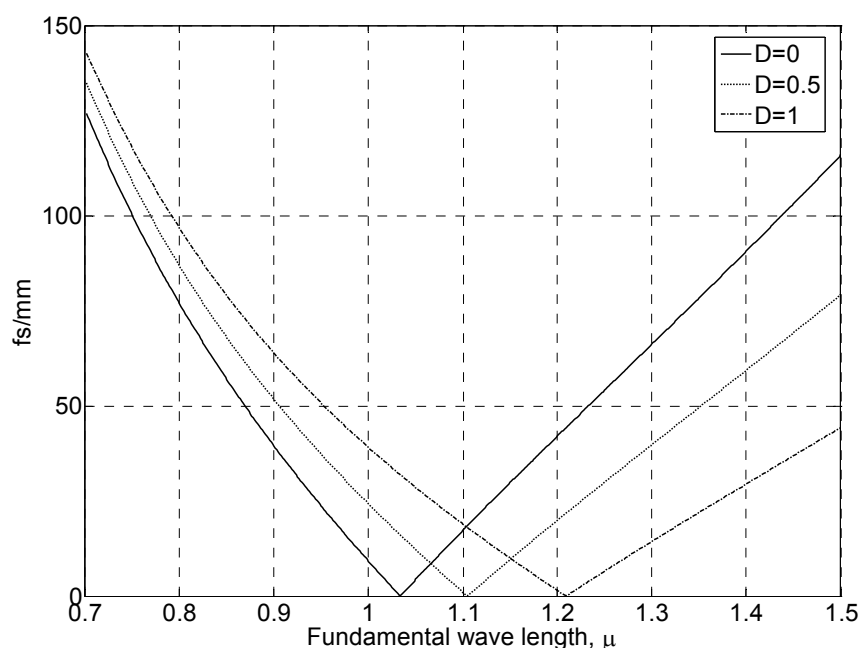


Fig. 2. Dispersion parameter P(λ) versus fundamental wave length at deuteration level D=0,0.5 and 1.

In order to verify theoretical model of SHG process under strong influence of cubic polarization effects we implemented modeling experiments. In the experiments we used output radiation of front end system of petawatt level femtosecond OPCPA laser (Lozhkarev, Freidman et al. 2007) as a fundamental beam. The parameters of the radiation incident on the SHG crystal (0.6 or 1.0mm thickness) were the following: beam diameter 4.3mm, pulse duration 65fs, energy range 1÷18 mJ, and central wavelength 910 nm. It is necessary to point out that the beam quality was not good, as a result at 18mJ energy the average over cross-section intensity was 2TW/cm² and the peak intensity was 5TW/cm². All measurements were done in vacuum, because for the range of fundamental intensities nonlinear beam self-action in air is important, even at several centimeters of propagation distance.

We have measured the energy efficiency of SHG in 0.6mm-thick KDP crystal at different detuning external angles Δθ, see fig.3. The main goal was to experimentally verify the fact that for efficient SHG different intensities require different optimal angles of beam propagation.

As can be seen from fig.3, a perfect phase matching (i.e. Δθ=0mrad) is optimal for SHG efficiency at low (2÷4mJ) and medium (10mJ) input energies. But at high energies (18mJ) SHG is more efficient at the optimal detuning angle Δθ=- 3.1mrad, because the phase induced by third-order nonlinearity and linear phase mismatching compensate each other. A negative value of optimal detuning angle is also clearly seen from comparison of data for Δθ=-6.2mrad and Δθ=6.2mrad: SHG efficiency is almost the same at 2-4mJ and is noticeably different at 16-18mJ. The experimental results are in a good agreement with formula (2), which gives for 18mJ energy (average intensity 2TW/cm²) Δθ=-3.5mrad.

Relatively low SHG efficiency and large spread of the experimental data are explained by poor quality of both the beam and the ultra thin KDP crystal. In a 1mm-thick KDP crystal we reached 41% of SHG energy efficiency at such high intensities.
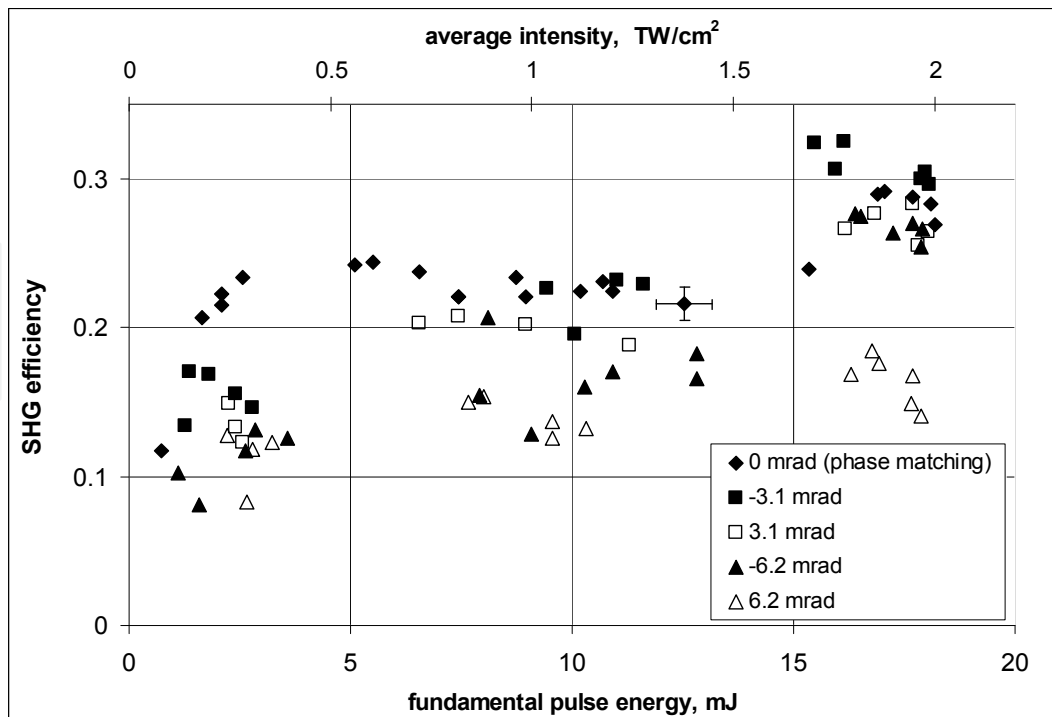
Fig. 3. The energy conversion efficiency *versus* input fundamental pulse energy at different detuning (external angles) from linear phase matching direction.

## 3. Pulse shortening and ICR enhancement

Cubic polarization leads to fundamental and second harmonic pulses spectrum modification and widening. The phenomenon depends on fundamental pulse intensity, cubic nonlinearity, fundamental central wave length and nonlinear element thickness. The output second harmonic pulse is not Fourier transform limited. In the case of optimal nonlinear element thickness, duration of second harmonic radiation approximately equals to the one of input pulse. Additional correction of spectrum phase of output second harmonic pulse makes it possible to significantly reduce pulse duration. The simplest way is the second order phase correction:

$$A_{2comp}(t) = F^{-1}\left[ e^{iS\omega^2} F\big[ A_2(z=L,t) \big] \right],$$

here $F$, $F^{-1}$ are the direct and inverse Fourier transforms, $A_2(z=L,t)$, $A_{2comp}(t)$ are the electric fields of second harmonic radiation before and after phase correction, and $S$ is the coefficient of quadratic spectral phase correction. The electric field $A_2(z=L,t)$ is obtained by the numerical solution of (1). The results are presented in fig.4 for optimal detuning angle $\Delta\theta$ (2) and for 5TW/cm$^2$ fundamental Gaussian pulse (20fs FWHM). The coefficient $S$ was chosen to minimize the pulse duration. Maximums of all the three pulses were shifted to zero time for clarity.

In accordance with fig.4, SHG process increases temporal ICR on pulse wings. Additional spectrum phase correction allows significantly reduce pulse duration. For instances, for fundamental wavelength Gaussian pulse with duration 20fs (FWHM) and intensity 5TW/cm$^2$, the second harmonic pulse may be compressed to 12fs (800nm, 0.2mm-thick
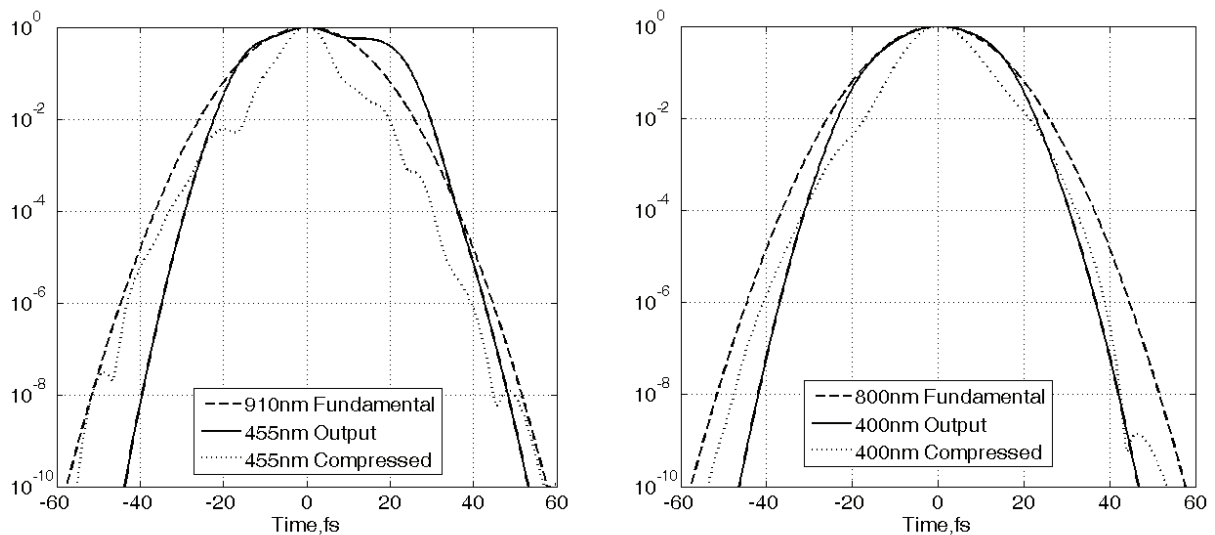
Fig. 4. Shapes of incident and second harmonic pulses before and after spectral phase correction. (a) fundamental wavelength 910 nm, KDP thickness 0.4 mm; (b) fundamental wavelength 800 nm, KDP thickness 0.2 mm.

KDP) and to 9fs (910nm, 0.4mm-thick KDP). The 50fs input pulse may be compressed even more efficiently in a 0.4mm-thick KDP: to 18fs at 800nm and to 16fs at 910nm.

The spectrum phase correction decreases ICR of second harmonic pulse in comparison with uncompressed, but it is higher than fundamental. As a result, SHG together with additional spectrum phase correction is suitable for peak intensity increasing and improvement of temporal intensity profile of super strong laser radiation.

## 4. Plane wave instability in mediums with quadratic and cubic nonlinearities

The other negative manifestation of cubic polarization is small-scale self-focusing (SSSF). The process is the main cause of laser beam filamentation and nonlinear element destructions. The theoretical aspects of the phenomenon in media with cubic polarization are observed in literature (Bespalov and Talanov 1966; Rozanov and Smirnov 1980; Lowdermilk and Milam 1981; Poteomkin, Martyanov et al. 2009). The main goal of the section is to develop theoretical approach to describe the process in media with quadratic and cubic nonlinearity. The model (Ginzburg, Lozhkarev et al. 2010) is necessary for estimations of critical level of spatial noise in super strong laser beams.

Let's assign three fundamental plane waves on the input surface of frequency doubling nonlinear element (waves 1, 3, 4 see fig 4). Angles $\alpha_1$ and $\alpha_2$ determine directions of harmonic disturbances of laser beam in non critical and critical planes of frequency doubling nonlinear element. Let's consider, that waves 3 and 4 has equal by amount, but anti directional transverse wave vectors. The wave 1 is significantly more powerful, than waves 3 and 4, and it runs in the optimal direction for energy conversion (in accordance with formula 2). Second harmonic wave (wave 2), which is generated by the wave number 1, runs at the same direction too.

Weak fundamental waves (3, 4) interact with strong waves (1, 2) and generate harmonic disturbances of second harmonic radiation (waves 5 and 6) see fig 4. The transversal wave vectors of fundamental and second harmonic waves should be equal. The requirement is a
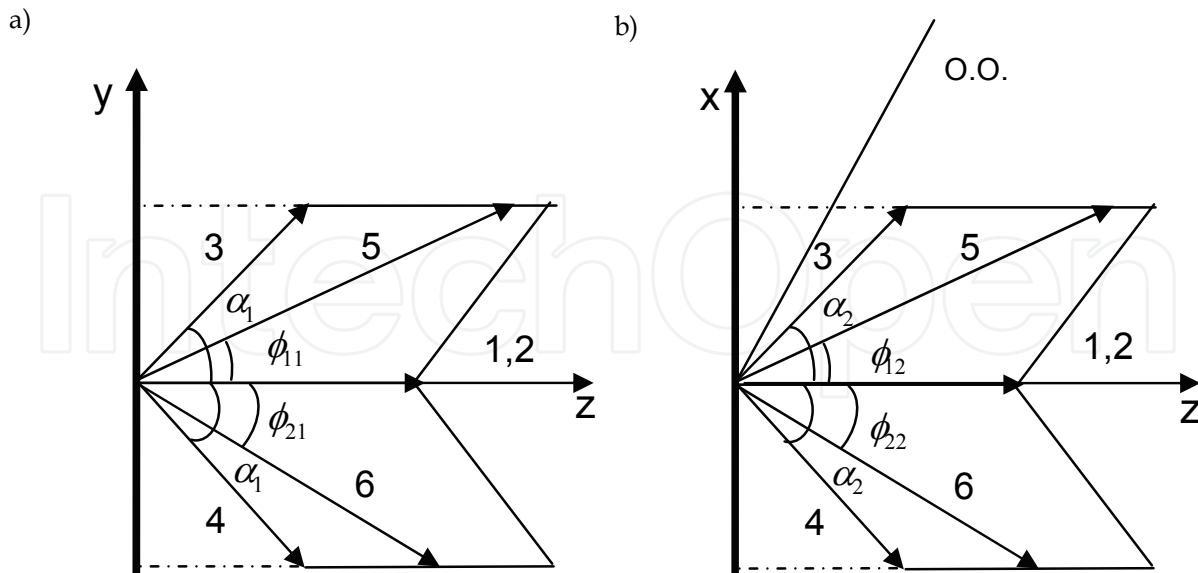
Fig. 4. The scheme of runs strong fundamental (wave 1) and second harmonic (wave 2) waves and their harmonic disturbances (waves 3,4 and 5,6 correspondingly) in non critical (a) and critical plane of frequency doubling nonlinear element.

consequence of Maxwell equations. The directions of second harmonic beam disturbances in non critical ($\phi_{11}, \phi_{21}$) and critical ($\phi_{12}, \phi_{22}$) planes are determined by boundary conditions (3):

$$
\begin{aligned}
&k_1 \sin(\alpha_2) = k_5 \sin(\phi_{12}) && k_1 \sin(\alpha_2) = k_6 \sin(\phi_{22}) \\
&k_1 \cos(\alpha_2)\sin(\alpha_1) = k_5 \cos(\phi_{12})\sin(\phi_{11}) && k_1 \cos(\alpha_2)\sin(\alpha_1) = k_6 \cos(\phi_{22})\sin(\phi_{21})
\end{aligned} \tag{3}
$$

So, the beam disturbances 3, 4, 5 and 6 have equal transversal wave vectors and their amplitudes satisfy the demands:

$$
|\varepsilon_i| << |\varepsilon_1|, |\varepsilon_2| \quad (i = 3..6) \tag{4}
$$

Assume, that on the boundary of the frequency doubling nonlinear element (z=0) the amplitudes of strong waves are the following:

$$
\varepsilon_1(z=0)=\varepsilon_{10} \text{ and } \varepsilon_2(z=0)=0 \tag{5}
$$

Here $\varepsilon_{10}$ – the electric field of the fundamental string wave (1). The conditions for harmonic disturbance amplitudes:

$$
\varepsilon_3(z=0) = \varepsilon_4(z=0) = \varepsilon_{30} \cdot e^{i\varphi}, \varepsilon_{5,6}(z=0) = 0, \tag{6}
$$

here $\varepsilon_{30}$ and $\varphi$ the initial electric strength of waves 3,4 and their phase on the entrance surface of nonlinear element. Assume, that amplification of harmonic disturbances is not crucial for strong wave interaction, i.e. amplitudes of wave 1 and 2 satisfy the system of differential equations:

$$\frac{d\varepsilon_1}{dz} = -i \cdot \beta \cdot \varepsilon_2 \cdot \varepsilon_1^* \cdot e^{-i\Delta k \cdot z} - i \cdot \gamma_{11} \cdot |\varepsilon_1|^2 \cdot \varepsilon_1 - i \cdot \gamma_{12} \cdot |\varepsilon_2|^2 \cdot \varepsilon_1,$$

$$\frac{d\varepsilon_2}{dz} = -i \cdot \beta \cdot \varepsilon_1^2 \cdot e^{i\Delta k \cdot z} - i \cdot \gamma_{21} \cdot |\varepsilon_1|^2 \cdot \varepsilon_2 - i \cdot \gamma_{22} \cdot |\varepsilon_2|^2 \cdot \varepsilon_2,$$
(7)

Now, observe mathematical description of plane wave instability in media with quadratic and cubic nonlinearity. Implementation of standard linearization procedure to quasi-optical equations, which describe dynamic of each frequency component, and grouping items with equal transverse wave vectors, gives opportunity to obtain equations for amplitudes of harmonic disturbances:

$$\frac{d\varepsilon_3}{dz} = \frac{-i}{\cos(\alpha_1)\cos(\alpha_2)}\left[\beta\left[E_1^*E_5 + E_4^*E_2\right] + \gamma_{11}\left[E_1^2E_4^* + 2|E_1|^2E_3\right] + \gamma_{12}\left[|E_2|^2E_3 + E_1E_2E_6^* + E_1E_5E_2^*\right]\right]e^{ik_1\cos(\alpha_1)\cos(\alpha_2)z}$$

$$\frac{d\varepsilon_4}{dz} = \frac{-i}{\cos(\alpha_1)\cos(\alpha_2)}\left[\beta\left[E_1^*E_6 + E_3^*E_2\right] + \gamma_{11}\left[E_1^2E_3^* + 2|E_1|^2E_4\right] + \gamma_{12}\left[|E_2|^2E_4 + E_1E_2E_5^* + E_1E_6E_2^*\right]\right]e^{ik_1\cos(\alpha_1)\cos(\alpha_2)z}$$
(8)

$$\frac{d\varepsilon_5}{dz} = \frac{-i}{\cos(\phi_{11})\cos(\phi_{12})}\left[2\beta E_3E_1 + \gamma_{21}\left[|E_1|^2E_5 + E_1E_2E_4^* + E_1^*E_2E_3\right] + \gamma_{22}\left[|E_2|^2E_6^* + 2|E_2|^2E_5\right]\right]e^{ik_5\cos(\phi_{11})\cos(\phi_{12})z}$$

$$\frac{d\varepsilon_6}{dz} = \frac{-i}{\cos(\phi_{21})\cos(\phi_{22})}\left[2\beta E_4E_1 + \gamma_{21}\left[|E_1|^2E_6 + E_1E_2E_3^* + E_1^*E_2E_4\right] + \gamma_{22}\left[|E_2|^2E_5^* + 2|E_2|^2E_6\right]\right]e^{ik_6\cos(\phi_{21})\cos(\phi_{22})z}$$

Here $E_i = \varepsilon_i e^{-ik_{zi}z}$, $k_1$– magnitude of fundamental wave vector, $k_5$, $k_6$ – wave vectors of second harmonic wave disturbances. In the frame of the model, the disturbances in the second harmonic beam appear from interaction between fundamental disturbances and strong fundamental wave (1). The second harmonic beam modulation is amplified over cubic polarization.

The amplification of harmonic disturbances depends on entrance fundamental intensity, quadratic and cubic nonlinearity, linear wave vectors mismatch, initial phase $\varphi$ on the entrance surface of frequency doubling media. The gain factors of fundamental and second harmonic disturbances can be determined $(i=3..6)$:

$$G_i(z,\alpha_1,\alpha_2,\varphi) = \frac{|\varepsilon_i(z,\alpha_1,\alpha_2,\varphi)|^2}{|\varepsilon_{30}|^2}.$$

As a rule, initial phase $\varphi$ is a random parameter, and hence the averaged gain factors are mostly interested in theoretical investigations:

$$G_{avi}(z,\alpha_1,\alpha_2) = \frac{1}{2\pi}\int_0^{2\pi} G_i(z,\alpha_1,\alpha_2,\varphi)d\varphi.$$

The averaged gain factors $G_{av1,2}$ versus harmonic disturbances propagation directions ($\alpha_1$, $\alpha_2$) are presented in fig.4 for 0.5mm KDP crystal, 4.5 TW/cm² fundamental intensity and assumption of optimal direction of beam propagation (in accordance with formula 2).

In accordance with fig 5, maximum of averaged by initial phase gain factors of fundamental and second harmonic disturbances, which were calculated for I=4.5 TW/cm² and 0.5mm KDP thickness, are the following $G_{av1}$=14, $G_{av2}$=270. Angular detuning in critical plane imposes restrictions on amplification of harmonic disturbances. As a result of it, angular
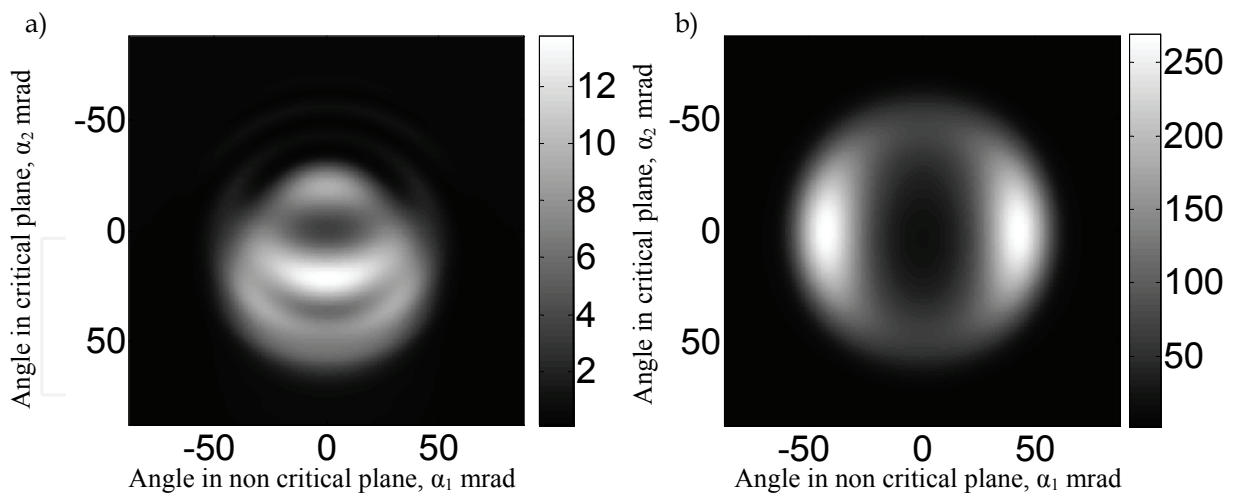
Fig. 5. The averaged gain factors of harmonic disturbances versus angles ($\alpha_1$, $\alpha_2$) a) $G_{av}$ fundamental and b) $G_{av}$ second harmonic. The diagrams were obtained by numerical solution of systems differential equations (7) and (8) with boundary conditions 5 and 6, KDP thicknesses 0.5mm and fundamental intensity I=4.5 TW/cm².

diagram in fig. 5 are symmetrical in non critical plane, i.e. $G_{avi}(z,-\alpha_1,\alpha_2)=G_{avi}(z,\alpha_1,\alpha_2)$ and non symmetrical in critical plane $G_{avi}(z,\alpha_1,-\alpha_2)\neq G_{avi}(z,\alpha_1,\alpha_2)$. Maximum amplification of harmonic disturbances of second harmonic wave (2) takes place at angles $\alpha_1$=42 mrad and $\alpha_2$=0 from direction of strong waves (1 and 2) propagation.

Note that for media with only cubic nonlinearity the gain factor can be found analytically (Rozanov and Smirnov 1980):

$$G_{th} = \frac{1}{4}\left(2\cosh^2(B_{11}x) + \left(\frac{2B_{11}x}{\kappa_1^2 - 4B_{11}}\right)^2 \sinh^2(B_{11}x) + \left(\frac{\kappa_1^2 - 4B_{11}}{2B_{11}x}\right)^2 \sinh^2(B_{11}x)\right),$$

here $B_{11}=\gamma_{11}A_{10}^2L$ is B-integral, $x^2 = \dfrac{\kappa_1^2}{B_{11}} - \dfrac{\kappa_1^4}{4B_{11}^2}$ , $\kappa_1 = k_{1\perp}\sqrt{L/k_1}$ - normalized transversal wave vector.

The other important parameter, which characterizes SSSF, is integral by spatial spectrum gain factor of harmonic disturbances. Let's determine it for the task by the following way:

$$G_{int_j} = \frac{1}{\pi\alpha_{cr}^2}\iint_{\Omega} G_{av_j} d\alpha_{j1} d\alpha_{j2}$$

here j=1,2 indexes of gain factors of noise amplification of fundamental and second harmonic wave, $\alpha_{cr}$ – angle in non critical plane, which corresponds to decreasing the gain factor of second harmonic disturbances in e times from the maximum value; $\Omega$ – is the circle of radius $\alpha_{cr}$ . Despite the complicated determination of the integral gain factors, they are physically enough, because it takes into account anisotropic topology of the gain structure (see fig.5). Calculated by the way integral gain factors for fundamental radiation I=4.5 TW/cm² and 0.5 mm KDP thickness are equal to $G_{int1}$=5, $G_{int2}$=107. Integral gain factors versus B-integral are presented in fig 6.
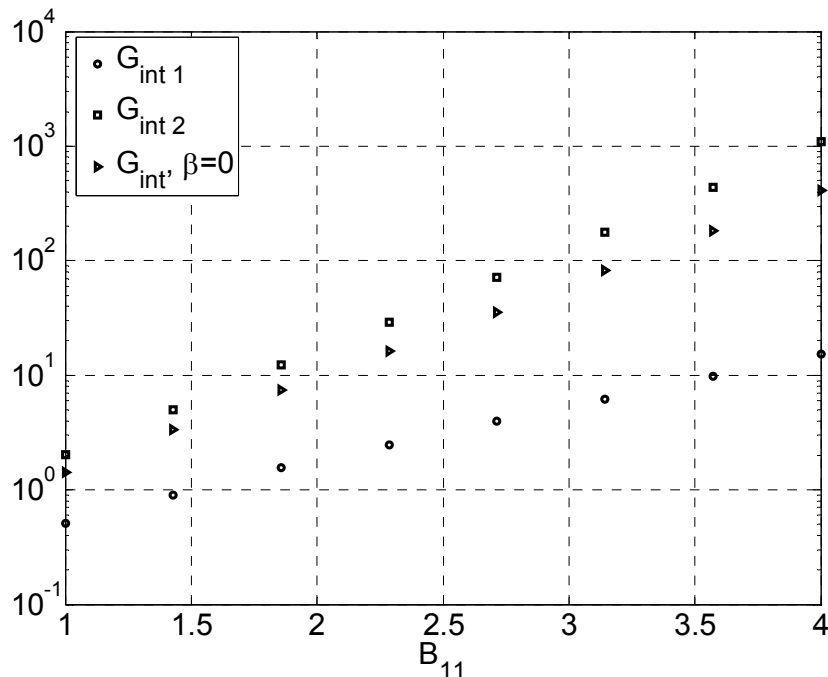
Fig. 6. Integral gain factors $G_{int1,2}$ fundamental and second harmonic disturbances versus B-integral

As can be seen from fig 6, the harmonic disturbances of fundamental and second harmonic waves are amplified significantly during second harmonic generation process. The fact can be a cause of a nonlinear element corruption.

Let's found critical level of spatial noise in the fundamental beam on the entrance surface of nonlinear element. Peak amount and mean square deviation intensity $I_{rms}$ from average in beam profile are connected with relative noise power $P_n/P$ by the following empiric formulas (Rozanov and Smirnov 1980):

$$I_{peak}/I_{av} = \left(1 + 5\sqrt{P_n/P}\right)^2$$
$$I_{rms}/I_{av} = \left(1 + \sqrt{P_n/P}\right)^2 - 1 \tag{9}$$

In accordance with (Kumar, Harsha et al. 2007), KDP crystal can stand under intensity about $I_{peak}$=18.5 TW/cm², 100fs pulse duration and central wave length $\lambda$=795 nm. Let's assume that the peak intensity is the threshold level for crystal destruction. In this case $K_{th} = I_{peak}/I_{av} = 4.1$ for average intensity $I_{av}$=4.5 TW/cm². Noise power on the output surface of frequency doubling nonlinear element can be found like $P_{nout} = G \cdot P_n$. Critical level of noise power $K_n = P_n/P$ of the fundamental entrance beam (by means of 9) is the following:

$$K_n = \frac{1}{G}\left(\frac{1}{5}\left(\sqrt{K_{th}} - 1\right)\right)^2.$$

For gain factor G=107 the amount is $K_n$=4 ·10⁻⁴ and $I_{rms}/I_{av} = 4 \cdot 10^{-2}$. The influence of SSSF effects can be diminished by means of beam quality improving and self filtering implementation, see next section.

## 5. Small-scale self-focusing suppression

The presented estimations of noise power critical level are overstated. The question is that, the observed theoretical model assumes the presence of high amplifying harmonic disturbances in nonlinear element and in the area of strong field. According to the observed theoretical model directions, where noise components start to be more intensive, depends on many factors such as fundamental intensity and central wave length, quadratic and cubic nonlinearity, direction of strong wave propagation with respect to optical axe, and thickness of frequency doubling nonlinear element. For fundamental intensity 4.5TW/cm² and 0.5mm KDP crystal the optimal angle for amplification of harmonic disturbance is 42 mrad (fig. 5). Such high angles make it possible to use free space propagation to cut off dangerous spatial components from strong light beam and there is no necessity to use spatial filters. The main sources of harmonic disturbances are mirror surfaces. Hence, the distance between the last mirror and nonlinear element is important parameter for spatial spectrum clipping (see fig 7).
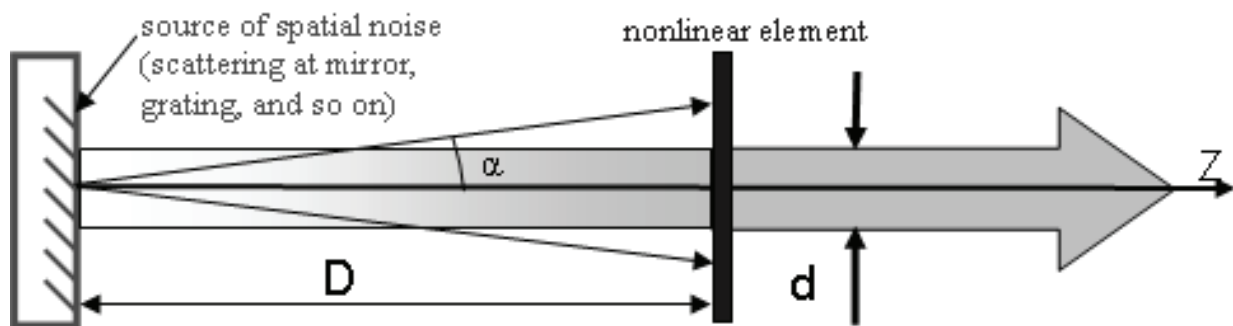


Fig. 7. The idea of small-scale self-focusing suppression. d is beam diameter, D is free-space propagation distance, α is angle of propagation of noise wave.

Differential equations 7 and 8 make it possible to find angle of optimal spatial noise increasing – $\alpha_{\max}$. The safety distance is $D \geq \dfrac{d \cdot \sqrt{1 - n^2 \cdot \sin^2(\alpha_{\max})}}{2 \cdot n \cdot \sin(\alpha_{\max})}$, there $d$ is the entrance beam diameter, $n$ – refractive index. This idea of small-scale self-focusing suppression by beam self-filtering due to free propagation before SHG may be used in any high intensity laser. The key parameters of the task are B-integral and angle of view $d/D$.

The power of noise on the entrance surface can be calculated by the following expression:

$$P_o = \iint_{\Omega} P_{\alpha o} d\alpha_1 d\alpha_2 = \pi \alpha^2 P_{\alpha o}$$

here $P_{\alpha o}$ – angular power density, $a_1$ и $a_2$ angles in non critical and critical plane, $\Omega$ – area in angular parameter space. On the entrance surface angular power density is homogeneous and the $\Omega$ is the circle with radius $a$ and center in the origin of coordinates. On the output surface the noise power is the following:

$$P_{out} = \iint_{\Omega} P_{\alpha o} G(\alpha_1, \alpha_2) d\alpha_1 d\alpha_2 = P_{\alpha o} \cdot \pi \cdot \alpha^2 \cdot G_{\text{int}}$$

Output noise power is proportional to $\alpha^2 \cdot G_{int}$. Maximum angle of integration is determined by the optical scheme geometry and refraction angle of frequency doubling nonlinear element.
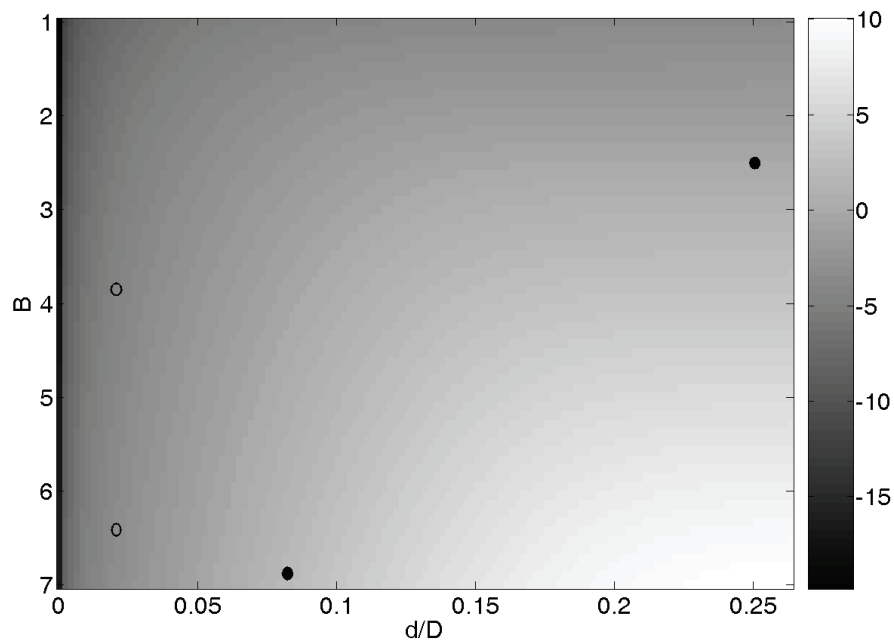


Fig. 8. Logarithm of normalized power of noise *ln(F)* versus B-integral and angle of view d/D at intensity 5TW/cm². Open circles show experiments without filamentaion and fill circles show experiment with filamentation.

The dependence of normalized power of the spatial noise $F=P_{out}(B,d/D)/\,P_{out}(B=2.5,\,d/D=1)$ at the output of nonlinear element is presented in fig. 8. At a large angle of view $d/D$ (no self-filtering) all noise waves reach the nonlinear element and noise power at its output is the highest. In this case filamentation appears at B≈2.5 (F≈1), the fact was observed in our experiments in accordance with other papers (Bespalov and Talanov 1966; Bunkenberg, Boles et al. 1981; Speck 1981; Vlasov, Kryzhanovskiĭ et al. 1982). When $d/D$ reduces to about 0.2 the noise power decreases as well. It drops sharply when $d/D$<0.1. As on can see from fig.3, experimental points with 0.6mm and 1mm thick crystal ($d/D$=0.02) are in a safety region: $F$<<1 even though B=3.8 and 6.4 correspondingly. On the other hand for experimental points where filamentaion was observed ($d/D$=0.08) the $F$ parameter is above unity, see fig.8.

Note, that in nanosecond lasers the typical intensity is 1GW/cm², hence, self-filtering takes place at the angle of view $d/D$<0.003, because the angle is proportional to the square root of laser beam intensity. Such a small value limits practical use of self-filtering for 1GW/cm² intensity laser pulses. The critical angle for medium with cubic nonlinearity only can be found in accordance with the following formula:

$$\alpha_{cr} = \sqrt{\frac{2\gamma I}{n}}$$

Here γ- cubic nonlinearity coefficient [cm²·watt⁻¹], I – intensity [cm⁻²·watt] and n - refractive index.

## 6. Surface dust influence to SHG process

Surface dusts are conductive to harmonic disturbance generation. The observed small-scale self-focusing suppression scheme can not be used for clipping spatial spectrum of noises, which are generated on surface. Generated on nonlinear element surface harmonic components have the same initial phase, which is equal to zero. The dynamic of plane wave instability can be described by system of differential equations 7 and 8. In this case boundary conditions are the following:

$$\varepsilon_1(z=0)=\varepsilon_{10}, \varepsilon_2(z=0)=0, \quad \varepsilon_{3,4}(z=0)=\varepsilon_{10}, \quad \varepsilon_{5,6}(z=0)=0$$

Gain factors versus of angles of harmonic disturbance propagation are presented in fig.9.
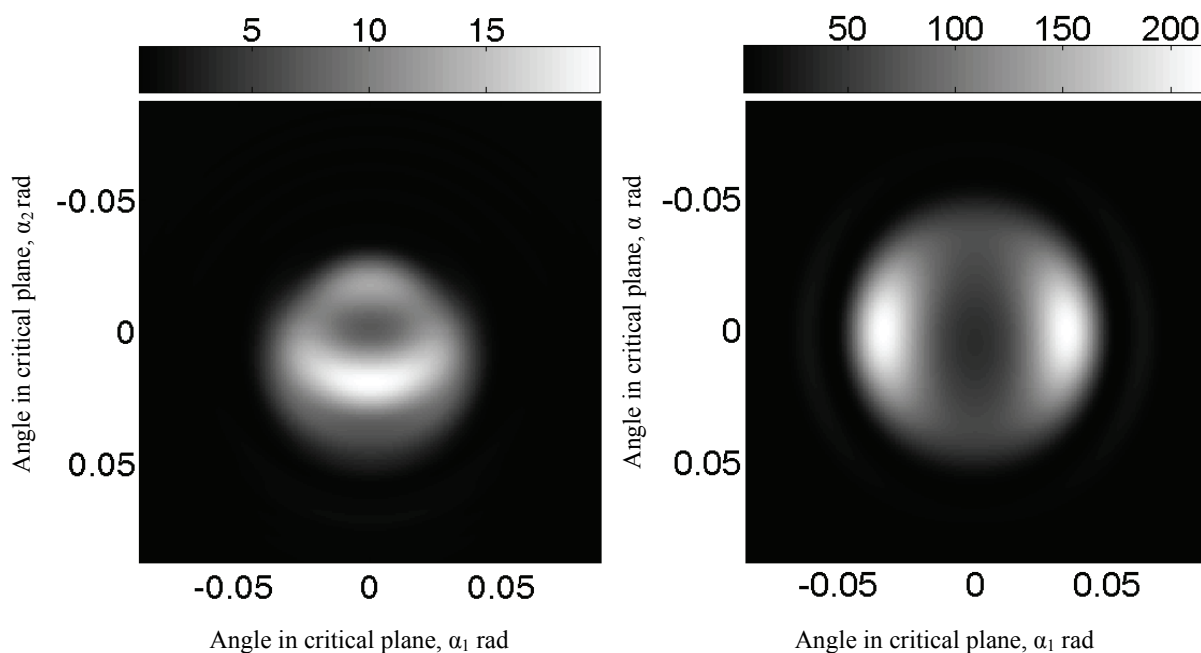


Fig. 9. Gain factors of harmonic disturbances a) fundamental and b) second harmonic waves. Calculated for 0.5mm KDP crystal and intensity 4.5TW/cm$^2$, angle of strong wave's propagation is optimal according to (2).

In accordance with fig.9 gain factors of harmonic disturbances of fundamental and second harmonic waves, which appears from scattering strong waves on surface dusts have topological structure the same to the averaged by initial phase gain factors. In this case preferable direction for noise amplification lies in non critical plane too. For fundamental intensity 4.5TW/cm$^2$ and 0.5mm KDP crystal the maximum gain factor of fundamental disturbances is 20, as for second harmonic noise it is 216 by optimal angle ±35mrad in non critical plane.

Thus, gain factors of harmonic disturbances of second harmonic wave, which is generated on surface dusts, are big sufficiently. In case of use of self-filtering technique described in Section 5, the input surface of SHG crystal is the main source of the noises. It is needed to be taken into consideration during experimental investigations.

## 7. Conclusion

We presented experimental conformation of theoretical model of SHG of super strong femtosecond radiation under strong influence of dispersion and cubic polarization effects. Despite the poor quality of the fundamental beam, the energy conversion efficiency of 35% (41%) was achieved in 0.6 (1.0) mm-thick KDP crystal.

SHG process is well for a increasing of temporal intensity contrast ratio significantly. The suggested additional spectrum phase correction of output second harmonic radiation is a way to reduce pulse duration more than 3 times for 50fs, $5TW/cm^2$ and 0.4mm KDP crystal. We demonstrated significant difference between 910nm and 800nm fundamental waves for SHG process and established the privilege of the first one.

The developed theoretical model of plane wave instability in mediums with quadratic and cubic nonlinearity makes it possible to estimate critical level of spatial noises power in super strong femtosecond laser beams for safety realization of SHG process. The suggested scheme of small-scale self-focusing suppression is theoretically explained and experimentally verified: no manifestation of self-focusing at B-integral above 6. The obtained experimental results are in a good agreement with the model. In the conclusion it is necessary to point out two additional sources of spatial noises as apply to SHG process. The first one is surface inhomogeneous and the second one is internal refractive index disturbances. The methodic of minimization of the factors is the improvement of nonlinear element quality: surface and homogeneity of refractive index.

## 8. References

Akhmanov, S. A., V. A. Vysloukh, et al. (1988). Optika femtosekundnykh lazernykh impul'sov. Moscow, Nauka.

Aoyama, M., K. Yamakawa, et al. (2003). "0.85-PW, 33-fs Ti:sapphire laser." Optics Letters 28(17): 1594-1596.

Bespalov, V. I. and V. I. Talanov (1966). "Filamentary structure of light beams in nonlinear liquids." JETP Letters 3: 307-310.

Bunkenberg, J., J. Boles, et al. (1981). "The omega high-power phosphate-glass system: design and performance." IEEE Journal of Quantum Electronics QE-17(9): 1620-1628.

Chien, C. Y., G. Korn, et al. (1995). "Highly efficient second-harmonic generation of ultraintense Nd:glass laser pulses." Optics Letters 20(4): 353–355.

Choe, W., P. P. Banerjee, et al. (1991). "Second-harmonic generation in an optical medium with second- and third-order nonlinear susceptibilities." J. Opt. Soc. Am. B 8(5): 1013–1022.

Ditmire, T., A. M. Rubenchik, et al. (1996). "The effect of the cubic onlinearity on the frequency doubling of high power laser pulses." J. Opt. Soc. Am. B 13(14): 649–655.

Ginzburg, V. N., V. V. Lozhkarev, et al. (2010). "Influence of small-scale self-focusing on second harmonic generation in an intense laser field." Quantum Electronics 40(6): 503-508.

Kochetkova, M. S., M. A. Martyanov, et al. (2009). "Experimental observation of the small-scale self-focusing of a beam in the nondestructive regime." Quantum Electronics 39(10): 923-927.

Kumar, R. S., S. S. Harsha, et al. (2007). "Broadband supercontinuum generation in a single potassium di-hydrogen phosphate (KDP) crystal achieved in tandem with sum frequency generation." Appl. Phys. B 86: 615-621.

Liang, X., Y. Leng, et al. (2007 ). "Parasitic lasing suppression in high gain femtosecond petawatt Ti:sapphire amplifier." Optics Express 15(23): 15335-15341.

Lowdermilk, W. H. and D. Milam (1981). "Laser-induced surface and coating damage." IEEE Journal of Quantum Electronics QE-17(9): 1888-1902.

Lozhkarev, V. V., G. I. Freidman, et al. (2007). "Compact 0.56 petawatt laser system based on optical parametric chirped pulse amplification in KD*P crystals." Laser Physics Letters 4(6): 421-427.

Lozhkarev, V. V., G. I. Freidman, et al. (2005). "Study of broadband optical parametric chirped pulse amplification in DKDP crystal pumped by the second harmonic of a Nd:YLF laser." Laser Physics 15(9): 1319-1333.

Mironov, S. Y., V. V. Lozhkarev, et al. (2009). "High-efficiency second-harmonic generation of superintense ultrashort laser pulses." Applied Optics 48(11): 2051-2057.

Poteomkin, A. K., M. A. Martyanov, et al. (2009). "Compact 300 J/ 300 GW frequency doubled neodimium glass laser. Part I: Limiting power by self-focusing." IEEE Journal of Quantum Electronics 45(4): 336-344.

Razumikhina, T. B., L. S. Telegin, et al. (1984). "Three-frequency interactions of high-intensity light waves in media with quadratic and cubic nonlinearities." Sov. J. Quantum Electron 14.

Rozanov, N. N. and V. A. Smirnov (1980). "Small-scale self-focusing of laser radiation in amplifier systems." Soviet Journal of Quantum Electronics 10(2): 232-237.

Speck, D. R. (1981). "The shiva laser-fusion facility." IEEE Journal of Quantum Electronics QE-17(9): 1599-1619.

Vlasov, S. N., V. I. Kryzhanovskiĭ, et al. (1982). "Use of circularly polarized optical beams to suppress selffocusing instability in a nonlinear cubic medium with repeaters " Soviet Journal of Quantum Electronics 12(1): 7-10.

Yanovsky, V., V. Chvykov, et al. (2008 ). "Ultra-high intensity- 300-TW laser at 0.1 Hz repetition rate." Optics Express 16(3): 2109-2114.
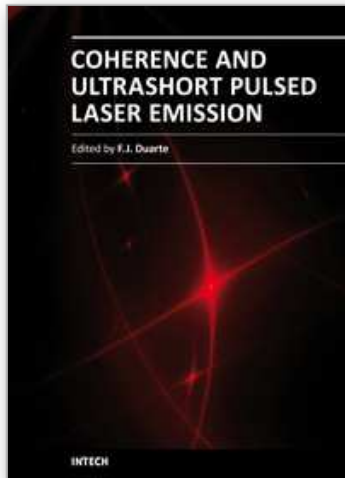
**Coherence and Ultrashort Pulse Laser Emission**

Edited by Dr. F. J. Duarte

In this volume, recent contributions on coherence provide a useful perspective on the diversity of various coherent sources of emission and coherent related phenomena of current interest. These papers provide a preamble for a larger collection of contributions on ultrashort pulse laser generation and ultrashort pulse laser phenomena. Papers on ultrashort pulse phenomena include works on few cycle pulses, high-power generation, propagation in various media, to various applications of current interest. Undoubtedly, Coherence and Ultrashort Pulse Emission offers a rich and practical perspective on this rapidly evolving field.

**How to reference**

In order to correctly reference this scholarly work, feel free to copy and paste the following:

# INTECH
open science | open minds